High Temperature Insulation Materials for DC Cable Insulation – Part I: Space Charge and Conduction

Mohamadreza Arab Baferani[1,2], Chuanyang Li[1], Tohid Shahsavarian[1,2], JoAnne Ronzello[1] and Yang Cao[1,2]

[1]Electrical Insulation Research Center, Institute of Materials Science
[2]Department of Electrical and Computer Engineering
University of Connecticut
Storrs, CT 06269, United States

ABSTRACT

Fundamental studies of potential candidates for DC electric power transmission in high temperature environment, including ETFE, FEP, PTFE, PI and PEEK, are carried out and presented in form of the series papers containing space charge and conduction as part I, partial discharge as part II, and the degradation and surface breakdown as part III. In this part, the space charge at 20kV/mm was measured at 25 °C and with a thermal gradient at 50 °C. The electrical conductivity was measured at electric fields ranging from 10kV/mm to 30kV/mm in temperatures ranging from 25 °C to 200 °C. The experimental results showed that considering the effect of thermal condition and electric field, FEP has the lowest total amount of space charge accumulation and electric field distortion among these materials at the measured conditions. PI and PEEK have the lowest amount of trap-controlled mobility at 25 °C due to deeper average trap level because of the aromatic rings in the structure. PTFE and PI have the lowest amount of thermal activation energy and temperature-dependent electrical conductivity due to the more uniform morphological phase comparing to ETFE, FEP, and PEEK. The outcomes of this paper serve as a benchmark for the fundamental researches over high temperature materials for DC applications and lay a basis for Part II and Part III.

Index Terms — **space charge measurement, electrical conductivity, activation energy, high temperature DC cable insulation**

1 INTRODUCTION

UNDERSTANDING the high temperature material behavior under DC voltage is an interesting study useful in a wide range of applications [1]. For DC power transmission under high temperature operation, the major challenge lies in figuring out the effect of temperature rise on the reliable operation of cable insulation. Because the electrical conductivity of insulation under DC electric field is temperature and electric field dependent, the spatial gradient of conductivity could lead to the accumulation of space charge in the bulk of cable insulation [2]. Moreover, space charge is easy to accumulate due to the bulk impurity ionization and charge injection at the electrode-dielectric interface at high temperature. Space charge can enhance electric field and increase the possibility of degradation and even catastrophic failure. Meanwhile, due to electric field distortion, partial discharge and local arc can result in material degradation, which may greatly reduce the insulation service life.

Manuscript received on 11 June 2020, in final form 24 September 2020, accepted 26 October 2020. Corresponding author: Y. Cao.

The effect of temperature rise and thermal gradient (TG) across the insulation on space charge formation and field enhancement is crucial in characterizing materials as DC cable insulation. Analyzing the effect of temperature gradient on the space charge accumulation inside of the bulk insulation has been conducted [3]. Chen *et al* have studied the space charge profiles and field distributions in low density polyethylene (LDPE) films under different temperature profiles, and DC stresses [4]. In [5], the effect of temperature on the conductivity of XLPE has been investigated. Also, Fu *et al* analyzed the effect of voltage reversal under TG on space charge [6]. However, all these materials can only be used in a temperature of lower than 150 °C, much lower than the operating temperature of 200 °C or even higher required for new aerospace applications.

For high temperature materials, Wang *et al* compared the mechanism of charge injection and accumulation of PE and PTFE [7]. In [8] and [9], the space charge accumulation of electron-beam irradiated fluorinated polymers (ETFE and FEP) and proton irradiated ones were studied, respectively.

DOI: 10.1109/TDEI.2020.009167

Also, authors of [10] studied the space charge of electron beam irradiated PI and PTFE with classical surface potential measurements and Pulse Electro-Acoustic (PEA). In [11], the authors compared the space charge distributions in electron-beam-irradiated FEP obtained with the laser induced pressure pulse (LIPP) and the laser-intensity-modulation-method (LIMM) methods. The space charge distribution in PI thin film was studies in [12] and the effect of space charge on breakdown of PI was investigated in [13]. However, very few researchers made a comparative study on different high-temperature insulating materials.

In this paper, the potential candidates for DC electric power transmission in high temperature environment, including Ethylene tetrafluoroethylene (ETFE), Fluorinated ethylene propylene (FEP), Polytetrafluoroethylene (PTFE), Polyimide (PI), and Polyether ether ketone (PEEK) are studied. These five materials represent the most important dielectrics used widely for high temperature applications for military, aerospace, marine, etc. Space charge was measured at 25 °C and with a TG at 50 °C, both at 20kV/mm, to understand the effect of temperature rise and TG condition on charge accumulation in the bulk of the materials. In addition, the conductivity was measured at 10, 20, and 30kV/mm and in the range of 25 to 200 °C. With this paper as a starter and also a basis, we have the second part focusing on partial discharge property under DC voltage for the high temperature materials [14] and the third part investigating degradation and surface flashover property of the same materials [15]. The content of this paper serves as references for the fundamental researches over high temperature materials and lays a basis for Part II and Part III.

2 EXPERIMENTAL

2.1 SAMPLE PREPARATION

The utilized materials are pure polymers of flat plaques, with thickness between 230–320 μm, i.e., PI 230 μm, ETFE, FEP and PTFE 250 μm, and PTFE 320 μm. All the samples are procured from Goodfellow. The samples are kept in the vacuum oven at room temperature to reduce the external effects including temperature, humidity, impurity, etc. on the samples.

2.2 EXPERIMENT DESCRIPTION

The space charge distribution was measured by a Pulsed Electroacoustic (PEA) instrument. Both sides of samples have been metalized with 60/40% gold/palladium. A small amount of silicone oil was applied on the semi-conductive electrode to improve the acoustic impedance matching. Pulse excitation of acoustic wave was achieved via the application of 350 V, 10 ns pulse generator with 1 ns rise time. The acoustic waves were detected by a polyvinylidene fluoride (PVDF) film sensor of 9 μm in thickness. The output of PEA system was recorded utilizing a Tektronix DPO5034 oscilloscope with 2.5 GS/sec sampling rate. The test chamber of the PEA system was housed inside an oven to control ambient temperature. To generate the TG across the thickness of the flat samples, four resistance heaters were placed on the bottom electrode to heat it up [16]. The resistance heaters were calibrated to provide ΔT=1.2 °C/mm TG for space charge measurements in this paper.

To measure the DC conductivity of bulk materials, a three-terminal sample holder was designed according to ASTM 257 Standard [17]. Samples were put in this guarded stainless-steel electrode system. An oven which can provide ambient temperature up to 200 °C was used and the experiment started after the preset temperature was stabilized for 20 minutes. The polarization current was recorded for 1000s by a Keithley 6514 electrometer and an average quasi steady state value from 900–1000s of the measurement was used to obtain the conductivity value.

3 EXPERIMENT RESULTS

3.1 SPACE CHARGE

Color maps in Figure 1 present the space charge distribution across the sample. The vertical axis describes the thickness of samples in per unit (P.U.). In this study, P.U. refers to the location of interest in the thickness direction of sample that is normalized to the total thickness of sample in which zero and one correspond to the positions of cathode and anode, respectively. The horizontal axis is representative of time during 120 minutes and colors correspond to the charge density in C/m^3. Figure 1(a) shows the space charge distribution of ETFE. ETFE presents small amount of negative charge close to the anode. The charge accumulation reaches 2.5 C/m^3 after 20 minutes of applying the voltage at 25 °C. The charge on the electrode-dielectric interface increases to 20 C/m^3 during a period of 8 minutes. At 50 °C with TG, as shown in Figure 1(b), the amount of space charge in the bulk increases to 5C/m^3 which is twice of the charge inside of the bulk at 25 °C, and the charge at the electrode-dielectric interface increases to 35C/m^3 which is about twice of the charge at the interface at 25 °C. Moreover, it takes longer time for the charge at the electrode-dielectric interface to reach the stable amount at 50 °C comparing to that of 25 °C. The location of the accumulated negative charge across the ETFE has a small shift at 50°C with TG compared to the measurement at 25 °C.

In Figure 1(c), the space charge in the bulk of FEP is less than 2 C/m^3 at 25 °C and the charge density at the electrode-dielectric interface increases to 25 C/m^3. At 50 °C after 40 minutes, the space charge inside of the bulk starts to appear, which is less than 3 C/m^3 and the charge density at the electrode-dielectric interface increases to 40 C/m^3 [Figure 1(d)]. Charge accumulation at the electrode-dielectric interface for FEP is quick, which takes less than 5 minutes to reach the stable amount. The space charge distributions in PTFE at 25 °C and at 50 °C with TG are demonstrated in Figures 1(e) and 1(f). As the results show, at 25 °C, negative space charge appears after 10 minutes next to the anode and in the middle of the bulk, which is less than 3 C/m^3. The charge at the electrode-dielectric interface reaches 25 C/m^3 in less than 5 minutes. At 50 °C, the amount of charge density inside of

the bulk does not change significantly and charge at the electrode-dielectric interface increases to 30 C/m^3.

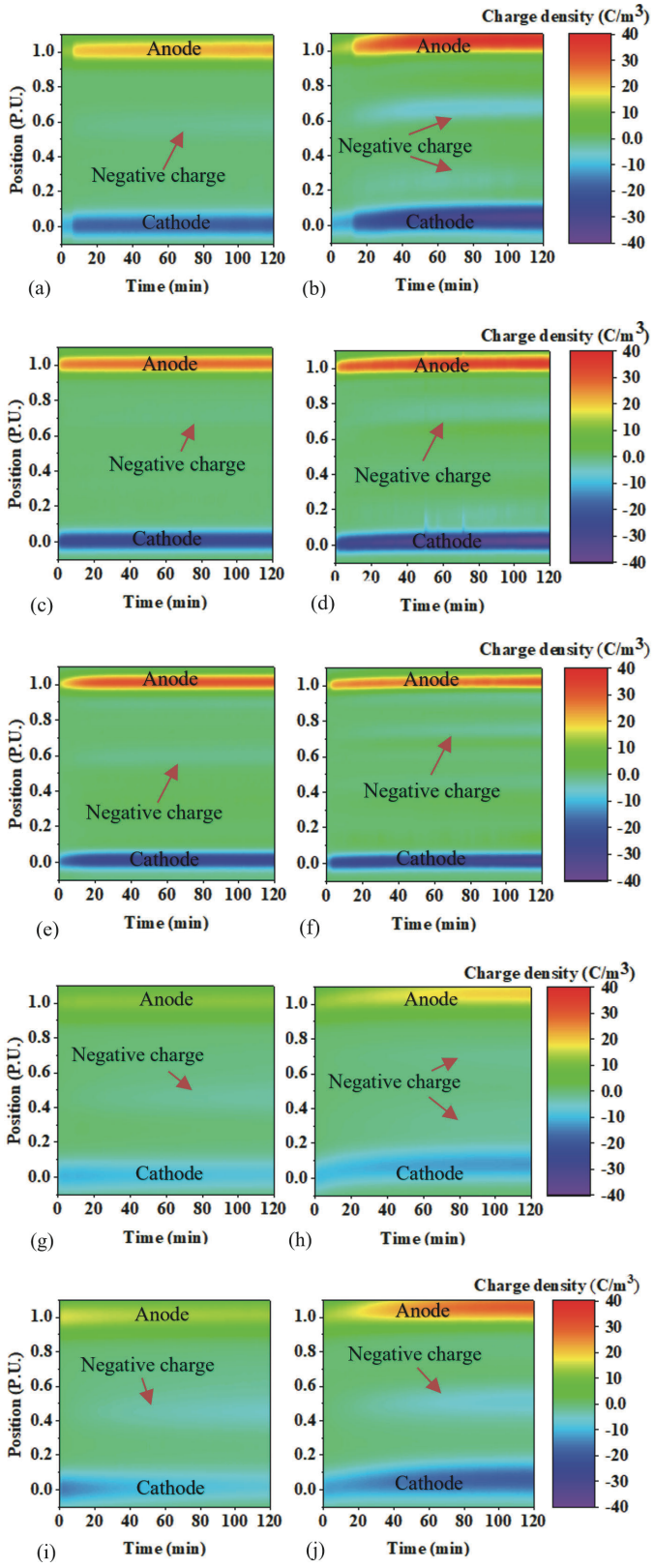

Figure 1. Space charge distributions under 20kV/mm. (a) ETFE at 25 °C, (b) ETFE at 50 °C with TG, (c) FEP at 25 °C, (d) FEP at 50 °C with TG, (e) PTFE at 25 °C, (f) PTFE at 50 °C with TG, (g) PI at 25 °C, (h) PI at 50 °C with TG, (i) PEEK at 25 °C, and (j) PEEK at 50 °C with TG.

The charge density distribution of PI, as shown in Figure 1(g), presents that at 25 °C, the negative space charge initiates after 20 minutes and charge at the electrode-dielectric interface reaches 10 C/m^3 quickly. At 50 °C [Figure 1(h)], the space charge inside of the bulk deceases, but the charge at the electrode-dielectric interface enhances to 35 C/m^3 after 60 minutes. For PEEK in Figure 1(i), after 20 minutes, negative space charge up to 5 C/m^3 appears in the middle of the bulk and charge at the electrode-dielectric interface reaches 15 C/m^3 rapidly and shows a slight decrease with time. At 50 °C, as presented in Figure 1 (j), the space charge initiates to enhance after 20 minutes at the same position with 25 °C and it increases up to 8C/m^3. The charge at the electrode-dielectric interface increases with time and reaches 25 C/m^3 for anode and 20C/m^3 for cathode.

From the experimental results represented in Figure 1, it can be observed that the location of charge accumulation for FEP and PEEK at 25 °C and 50 °C is the same location although the fresh sample has been used for each measurement. For ETFE, PTFE and PI a slight shift in the location of the accumulated negative charge at 50 °C with TG compared to 25 °C can be seen.

3.2 ELECTRIC FIELD DISTRIBUTION

The electric field distribution across the materials was calculated based on the charge density distribution. Without any space charge accumulation, the electric field distribution across a plaque sample is uniform, but presence of accumulated charge would distort electric field and lead to local electric field enhancement. Figure 2 depicts the electric field distribution of the materials under 20 kV/mm at 25 and 50 °C with TG during 120 minutes. To clarify the evolution of electric field more clearly, only electric field distributions at first second and after 60 and 120 minutes were presented.

As it can be observed, electric field at first second for all the materials is uniform at 20 kV/mm. After 60 minutes, the electric field distribution across the sample has been distorted and local electric field enhancement depending on the position of accumulated charge can be seen. All materials have electric field enhancement next to the anode at 25 °C and at 50 °C with TG although it is more considerable in PEEK and PI. For PTFE, the electric field enhancement next to both electrodes can be seen at 50 °C.

3.3 CONDUCTIVITY

Figure 3 shows the result of electrical conductivity of all the samples at 10, 20, and 30 kV/mm, each at 25, 50, 100, 150, and 200 °C, respectively. At 25 and 50 °C, the electrical conductivity of all the materials at different electric fields are in the range of 10^{-15} to 10^{-14}(S/m). PI shows the highest electrical conductivity at 25 °C under 10, 20 and 30 kV/mm and at 50 °C under 20 and 30 kV/mm. With temperature rise above 50 °C, the intensity of electrical conductivity is more distinct. For instance, the range of the electrical conductivity for PEEK and ETFE is 10^{-11} to 10^{-8}(S/m), for FEP and PI is 10^{-13} to 10^{-11}(S/m), and for PTFE 10^{-14} to 10^{-13}(S/m). At 100 °C and 150 °C, ETFE has the highest electrical conductivity

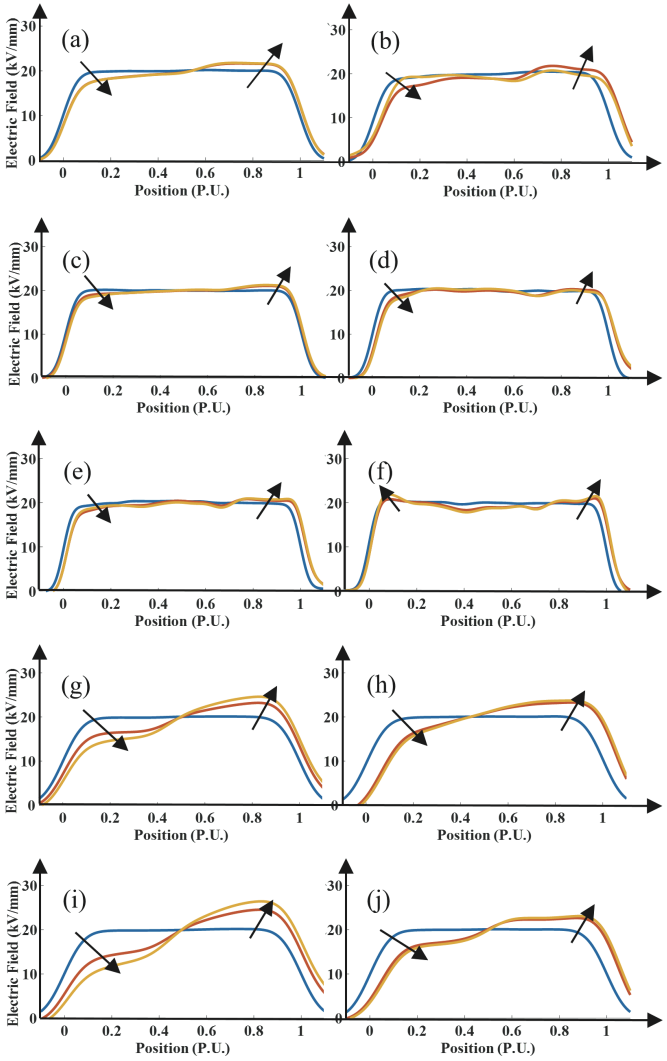

Figure 2. Electric field distributions under 20kV/mm for: (a) ETFE at 25 °C, (b) ETFE at 50 °C with TG, (c) FEP at 25 °C, (d) FEP at 50 °C with TG, (e) PTFE at 25 °C, (f) PTFE at 50 °C with TG, (g) PI at 25 °C, (h) PI at 50 °C with TG,(i) PEEK at 25 °C, and (j) PEEK at 50 °C with TG.

under 10, 20, and 30 kV/mm. It shows clearly the increase of electrical conductivity in ETFE from 50 to 200 °C. At 200 °C, PEEK exhibits an electrical conductivity close to ETFE under 10 kV/mm, but higher than ETFE under 20 and 30 kV/mm.

For the step of temperature rise from 25 to 50 °C, all materials have a slight decrease in electrical conductivity except for PEEK under 10 and 20 kV/mm as well as for PI under 30 kV/mm. This may be due to the possible presence of moisture inside of the materials from the manufacturing process. After 50°C with the increase of temperature to 200 °C, the electrical conductivity of all materials was enhanced with different slopes. In general, the increase of electrical conductivity for PTFE is the least while for PEEK is the most. The rate of electrical conductivity enhancement and the range of temperature for maximum slope of change are different for the materials. ETFE, FEP, and PI have the maximum electrical conductivity growth in the range of 50 to 150 °C, but for PEEK this increase is highest in the step of 150 to 200 °C. PTFE shows more uniform slope from 50 to

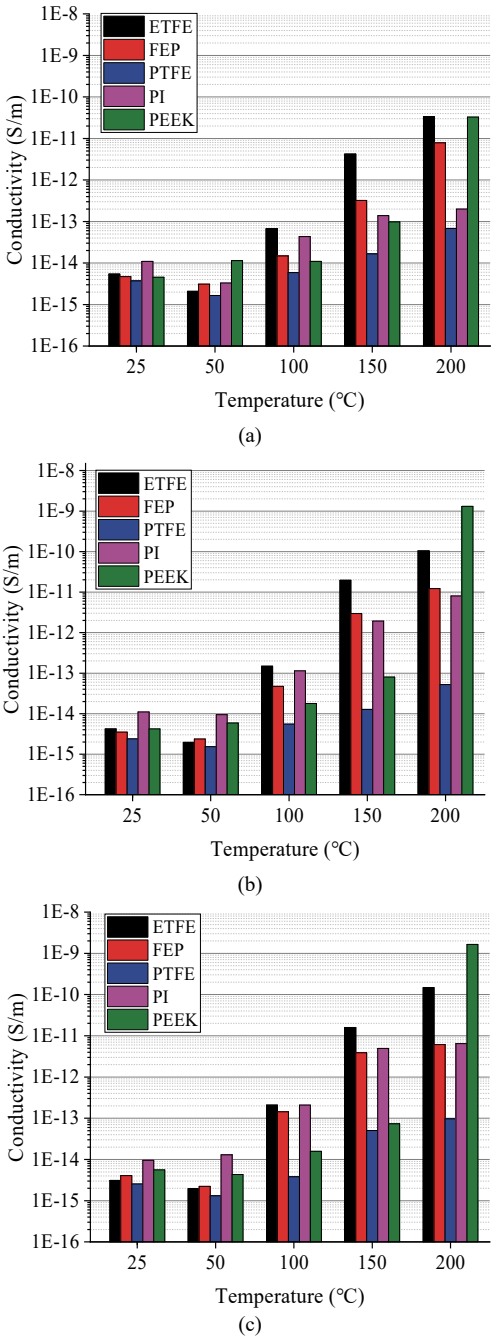

Figure 3. Conductivity in the range of 25 °C to 200 °C under different electric field: (a) 10 kV/mm, (b) 20 kV/mm, and (c) 30 kV/mm.

200 °C comparing to the other materials investigated. It shall be noted that both PI and PEEK contain conjugating aromatic ring structures with π-bonds, while ETFE, FEP and PTFE are all family members of full or partial fluorocarbons with σ-bonding chains.

4 DISCUSSION

4.1 SPACE CHARGE AND ELECTRIC FIELD DISTORTION

Space charge accumulation can distort electric field distribution, which may lead to potential breakdown of insulation. However, not all kinds of charge accumulation can

have a significant impact on breakdown while this impact can become larger at high temperatures [18, 19]. In this part, the relation between space charge accumulation and electric field distortion under temperature rise and TG is discussed. In general, the testing temperature has significant effects on space charge dynamics like enhancement of ionic dissociation, charge injection, charge mobility and electrical conductivity of dielectrics. To clarify the effect of increasing temperature on charge density at the electrode-dielectric interface and in the bulk, the maximum charge density during polarization time has been plotted in Figure 4 for further discussion.

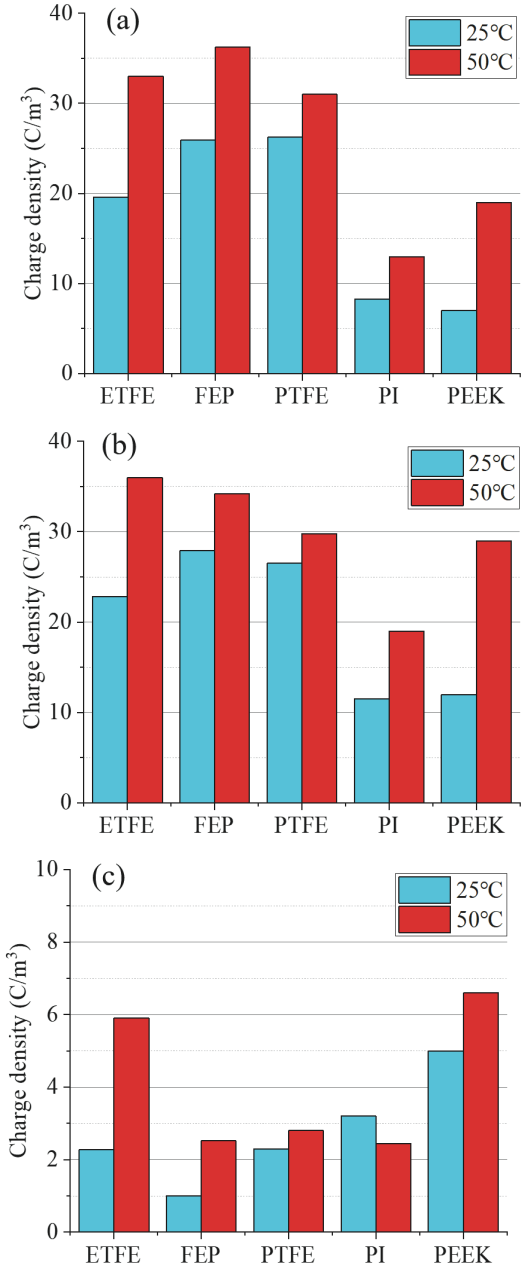

Figure 4. Maximum charge density: (a) at the negative electrode-dielectric interface, (b) at the positive electrode-dielectric interface, (c) inside of the bulk.

As it can be seen from Figures 4(a) and 4(b), the charge density at the electrode-dielectric interface of all the materials enhances with the increase of temperature in both polarities. This states that charge injection enhances with raising the temperature in both polarities and the injected electrons and holes are trapped at the electrode-dielectric interfaces. Considering both polarities, charge density at the electrode-dielectric interface of PTFE has the least enhancement which shows less change in charge injection with temperature rise for this material.

Moreover, the maximum trapped charge density inside of the bulk during 120 minutes has been presented in Figure 4(c) which is negative charge. At 25 °C, the maximum of space charge for PI and PEEK are higher than ETFE, FEP and PTFE. Considering the charge density at the electrode-dielectric interfaces, it seems that the injected electrons from the cathode were transported across the sample and captured by traps. The aromatic structures of PI and PEEK might provide deep traps which result in the enhanced amount of trapped charge in the bulk at 25 °C [20, 21].

With the temperature rise, the maximum trapped charge inside of the bulk for ETFE, PEEK and FEP have observable enhancement. The maximum charge density changes slightly for PI and PTFE. It means that change of charge density inside of the sample for PI and PTFE is less dependent on the temperature rise in the range of 25 °C to 50 °C. This should be correlated to the morphology of these materials. In Section 4.3, the reason for this observation would be discussed with more details.

To understand and compare the results of electric field distortion due to space charge accumulation with temperature rise, maximum electric field (MEF), E_{max}, and MEF enhancement (MEFE) factor, f, are used as two indices:

$$f = \frac{E_{max} - E_{DC}}{E_{DC}} \times 100\% \quad (1)$$

where E_{max} is MEF and E_{DC} is the nominal electric field and f is MEFE factor in percentage.

The MEF and f for the materials have been depicted in Figures 5(a) and 5(b), respectively. Comparing all the materials, FEP with MEF of 21.1 kV/mm at 25 °C and 20.5 kV/mm at 50 °C with TG and MEFE of less than 10% has the lowest electric field distortion. On the other hand, PEEK shows the maximum electric field enhancement of 26 kV/mm and 23.1 kV/mm at 25 °C and 50 °C, respectively. PTFE has the MEF of 22.9 kV/mm at 25 °C and 23 kV/mm at 50 °C which are almost equal.

By comparing the calculated electric field distribution, the MEF of all the materials except PTFE decreased at 50 °C with TG. For ETFE, FEP, PI, and PEEK, the charge density at the electrode-dielectric interfaces increased more severely as shown in Figures 4(a) and 4(b) compared to the charge enhancement inside of the bulk, Figure 4(c). This possibly implies that although the charge injection increases with temperature rise, the major part of the injected charge was trapped at the electrode-dielectric interfaces and the minor part of that was trapped inside of the bulk when they were moving across the sample.

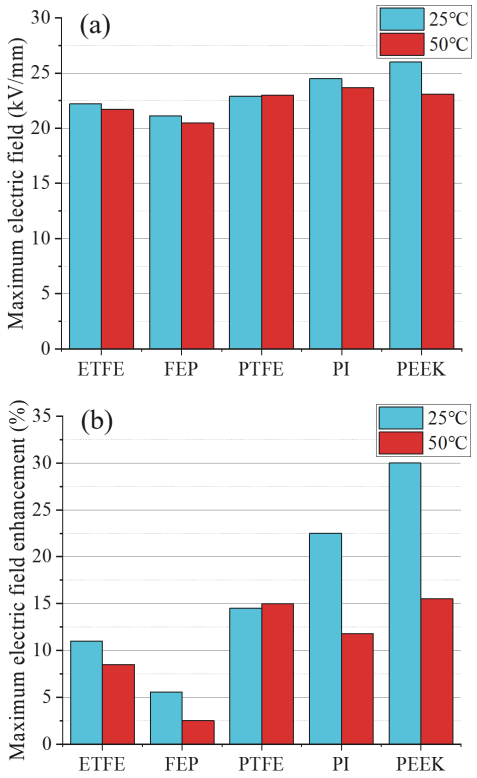

Figure 5. (a) Maximum electric field, and (b) maximum electric field enhancement under 20 kV/mm at 25 and 50 °C.

This alteration in maximum electric field across the sample can be the result of the ratio of charge density in the bulk to the charge density at the electrode-dielectric interface. Moreover, the position of charge accumulation across the sample can influence the amount and position of electric field enhancement. Considering the results of space charge accumulation and calculated electric field distribution at 25 and 50 °C, FEP has the best performance among the 5 different materials. As well, ETFE and PEEK show the worst space charge accumulation among these materials at 25 and at 50 °C with TG.

4.2 DEPOLARIZATION, MOBILITY AND TRAP LEVEL

Space charge accumulation is the result of trapping of charge carriers in shallow and deep traps inside of the bulk. In addition to the charge accumulation, transport and dissipation of charge carriers are in relation with the trapping and de-trapping processes of charge carriers [22]. When the traps are deep, the charge carriers would spend longer time in the traps and it decreases the mobility of charge carriers. As a result, the depolarization measurement after polarizing process and calculation of the apparent trap-controlled mobility could provide a rough approximation of mobility of trapped charge carriers [23] and it is useful for material characterization. To reach the trap-controlled mobility, the space charge under depolarization process was recorded for 30 minutes after 120 minutes polarizing at 25 °C. The apparent trap-controlled mobility, $\mu(t)$, can be calculated by using Equation (2) and having $q(t)$ which is the average of charge density with time, t [24].

$$\mu(t) = \frac{2\varepsilon}{q(t)^2}\frac{dq(t)}{dt} \tag{2}$$

Furthermore, trap level depth can be estimated by Equation (3) [24]:

$$\varphi(t) = k_B T ln(\mu \frac{kT}{\nu e R^2}) \tag{3}$$

in which k_B is the Boltzmann constant, R is the mean distance between localized states (5×10^{-7}), e is the electron charge, $\nu = kT/h$ is the attempt to escape frequency and h is the Planck constant.

Table 1 presents the average of trap-controlled mobility and trap level depth based on depolarization measurement for the materials polarized under 20 kV/mm during 1500 s at 25 °C after 120 minutes polarization.

Table 1. The average of trap-controlled mobility and trap level depth of materials for 1500s.

Materials	Trap-controlled mobility ($m^2/(V\cdot s)$)	Trap level (eV)
ETFE	2.90×10^{-12}	0.733
FEP	6.67×10^{-12}	0.739
PTFE	3.84×10^{-12}	0.734
PI	9.17×10^{-14}	0.749
PEEK	1.83×10^{-13}	0.756

As it can be seen, the trap-controlled mobility of charge carriers for ETFE, FEP, and PTFE are in the range of 10^{-12} $m^2/(V\cdot s)$ and higher than PI and PEEK. PI with the trap-controlled mobility of 9.17×10^{-14} $m^2/(V\cdot s)$ has the lowest mobility among these materials. In addition, the average of trap level of ETFE, FEP, and PTFE in comparison to PI and PEEK are lower. This is due to the aromatic rings in the backbone of PI and PEEK structure which can enhance the depth of traps and lead to the reduction in trap-controlled mobility [19]. In other words, the depolarization process is slower for PI and PEEK than ETFE, FEP and PTFE, because the average trap level for PI and PEEK is higher and the trapped charge would stay longer in the traps.

4.3 THERMAL ACTIVATION ENERGY

The space charge measurement from PEA instrument shows the total accumulated space charge. The measured space charge can be due to the conductivity gradient across of the dielectric, ionization of the impurities, and charge carrier injection. The space charge as a result of the conductivity gradient can be calculated by the following equation [2]:

$$\rho = -\frac{-\varepsilon_0\varepsilon_r}{\sigma}\frac{\partial\rho}{\partial t} + \sigma E.\nabla\left(\frac{\varepsilon_0\varepsilon_r}{\sigma}\right) \tag{4}$$

where ρ is the generated space charge (C/m^3), σ is electrical conductivity (S/m), E is the electric field (V/m), ε_r is dielectric constant and ε_0 is the permittivity of vacuum.

Because of the fact that dielectric permittivity is not strongly dependent on temperature, the temperature coefficient of the electrical conductivity and its gradient are responsible for the aforementioned part of space charge formation as in Equation (4). As a result, the low dependency of the electrical conductivity to temperature and hence a reduced electrical conductivity gradient can reduce the space charge formation.

The electrical conductivity is a function of electric field and temperature for polymer dielectrics with an Arrhenius type relationship [25]:

$$\sigma(T) = \sigma_0 \exp\left(\frac{-\varphi q}{k_B T}\right) \quad (5)$$

where σ_0 is the base conductivity, φ is the thermal activation energy, q is the electronic charge, and T is the absolute temperature. This equation can be utilized to fit the experimental results to calculate the activation energy of materials. The activation energy indicates the dependency of the material's electrical conductivity to the temperature rise. The higher the activation energy, the more temperature-dependent the electrical conductivity becomes. Table 2 presents the calculated activation energy by fitting the experimental results of electrical conductivity with Equation (5) at three different electric fields of 10, 20, and 30 kV/mm.

Table 2 Activation energy of the materials at different electric fields.

Materials	Activation energy (eV)		
	10kV/mm	20kV/mm	30kV/mm
ETFE	0.262	0.304	0.323
FEP	0.223	0.245	0.220
PTFE	0.087	0.092	0.109
PI	0.087	0.198	0.195
PEEK	0.267	0.380	0.378

As it can be understood from the activation energy results, the conductivity of PTFE and PI with 0.087 eV activation energy at 10 kV/mm has the lowest dependency to temperature and PEEK has the highest activation energy with 0.267 eV at 10kV/mm which shows its direct dependency to temperature comparing to the other materials. The low activation energy of PTFE and PI especially at 10 kV/mm, which is close to the electric field of DC power cables at normal operational condition, makes them proper candidates in terms of electrical conductivity. Moreover, it can be seen that generally the activation energy of materials increases with electric field rise although the activation energy at 30 kV/mm is less than 20 kV/mm for FEP, PEEK and PI. It appears that under higher electric field the electrical conductivity becomes more temperature-dependent.

To understand the possible reason for the difference in activation energy, it should be considered that the level of crystallinity is an important parameter in electrical conductivity of polymeric insulations. ETFE, FEP, and PEEK are semi-crystalline with different level of crystallinity, but PI is highly amorphous and PTFE is highly crystalline. The level of crystallinity has large effect on the trap level and the trap distribution of polymers and can influence the electrical conductivity of materials. It can be stated that on the interface of crystalline and amorphous phase, the charge carriers face the energy barriers which block the charge transport inside of the bulk. As a result, at the interface of crystalline and amorphous phase of the semi-crystalline dielectrics, the density of trap distribution is higher and it is more dependent on temperature. This fact can determine the temperature-dependency of conductivity of the materials. PTFE is highly crystalline and PI is highly amorphous and the reason of the lower activation energy of these materials is their uniform phase. In other words, the trap density of these materials is not dependent on temperature significantly. On the other hand, ETFE, FEP and PEEK are semi-crystalline and this causes that the electrical conductivity of these materials are temperature-dependent and the activation energies are higher. In Section 4.1, it was mentioned that the maximum negative charge density of PTFE and PI has less change when temperature rises from 25 to 50 °C. This also can be due to the less dependency of the trap density of PTFE and PI to temperature since their morphological phase is more uniform.

5 CONCLUSIONS

In this paper, five main candidates for utilizing as DC cable insulation for high temperature application, ETFE, FEP, PTFE, PI and PEEK, have been studied. The main conclusions are as follows:

(1) From 25 to 50°C, the space charge density at the electrode-dielectric interface of all the materials enhances which presents charge injection enhancement with temperature rise. As well, the electrical conductivity grows with temperature rise especially from 50 to 200 °C, although the dependency of electrical conductivity to temperature is considerably different among the materials.

(2) FEP presents the lowest space charge accumulation and electric field distortion across the film sample polarized under 20 kV/mm at both 25 and 50 °C with TG, while PEEK shows the highest amount of space charge at the same conditions.

(3) From the depolarization characterization at 25 °C, the average of trap level for PEEK and PI are higher compared to ETFE, FEP, and PTFE. Deeper trap levels of PI and PEEK lead to lower trap-controlled mobility for these materials.

(4) PTFE and PI have the lowest activation energy and the electrical conductivity of these materials has the least dependency on temperature.

REFERENCES

[1] Y. Tanaka *et al*, "Space Charge Accumulation Properties in Various Insulating Materials under DC High Electric Field at High Temperature," *IEEE Int. Conf. Electr. Mat. Power Equip. (ICEMPE)*, 2019, pp. 22–30.

[2] B. X. Du, C. Han, J. Li, and Z. Li, "Effect of voltage stabilizers on the space charge behavior of XLPE for HVDC cable application," IEEE Trans. Dielectr. Electr. Insul., vol. 26, no. 1, pp. 34–42, Feb. 2019.

[3] D. Fabiani *et al*, "HVDC cable design and space charge accumulation. Part 3: Effect of temperature gradient," IEEE Electr. Insul. Mag., vol. 24, no. 2, pp. 5–14, 2008.

[4] X. Chen *et al*, "Effect of voltage reversal on space charge and transient field in LDPE films under temperature gradient," IEEE Trans. Dielectr. Electr. Insul., vol. 19, no. 1, pp. 140–149, 2012.

[5] L. Lan *et al*, "Effect of temperature on space charge trapping and conduction in cross-linked polyethylene," IEEE Trans. Dielectr. Electr. Insul., vol. 21, no. 4, pp. 1784–1791, 2014.

[6] M. Fu *et al*, "Space charge formation and its modified electric field under applied voltage reversal and temperature gradient in XLPE cable," IEEE Trans. Dielectr. Electr. Insul., vol. 15, no. 3, pp. 851–860, 2008.

[7] W. Wang *et al*, "Space charge mechanism of polyethylene and polytetrafluoroethylene by electrode/dielectrics interface study using quantum chemical method," IEEE Trans. Dielectr. Electr. Insul., vol. 24, no. 4, pp. 2599–2606, 2017.

[8] M. Miyoshi *et al*, "Charge accumulation characteristics of fluorine insulating materials under electron beam irradiation," *IEEE Int. Symp. Electr. Insul. Mat. (ISEIM)*, 2017, pp. 508–511.
[9] H. Miyake *et al*, "Space charge accumulation behavior in fluorinated polymer films irradiated by proton under DC stress," *Annu. Rep. Conf. Electr. Insul. Dielectr. Phenom. (CEIDP)*, 2017, pp. 50–53.
[10] C. Perrin *et al*, "Space Charge Detection in Kapton® and PTFE Polymer Films by the Open Pulsed Electro-Acoustic Method," High Performance Polymers, vol. 20, no. 4–5, pp. 535–548, 2008.
[11] A. Mellinger and R. Singh, "A comparison of space-charge distributions in electron-beam irradiated FEP obtained by using heat-wave and pressure-pulse," J. Appl. Phys., vol. 30, no.11, pp. 1668–1675, 1997.
[12] C. Pham *et al*, "Space charge distributions in Polyimide thin films determined by FLIMM," *Annu. Rep. Conf. Electr. Insul. Dielectr. Phenom. (CEIDP)*, 2011, pp. 121–124.
[13] Y. Muramoto *et al*, "Space charge distribution of polyimide films in high temperature region," *Annu. Rep. Conf. Electr. Insul. Dielectr. Phenom. (CEIDP)*, 1999, vol. 1, pp. 110–113.
[14] T. Shahsavarian *et al*, "High Temperature Insulation Materials for DC Cable Insulation – Part II: Partial Discharge", IEEE Trans. Dielectr. Electr. Insul., accepted.
[15] C. Li *et al*, "High Temperature Insulation Materials for DC Cable Insulation – Part III: Degradation and Surface Breakdown", IEEE Trans. Dielectr. Electr. Insul., accepted.
[16] M. A. Baferani *et al*, "Study of space charge behavior of insulations for high temperature applications," *Annu. Rep. Conf. Electr. Insul. Dielectr. Phenom. (CEIDP)*, 2019, pp. 490–494.
[17] Standard Test Methods for DC Resistance or Conductance of Insulating Materials, ASTM Standard D257-07, 2007-05-15.
[18] Z. Li, *et al*, "Inhibition Effect of Graphene on Space Charge Injection and Accumulation in Low-Density Polyethylene," Nanomaterials, vol. 8, no. 11, pp. 956, 2018.
[19] C. Li *et al*, "Charge cluster triggers unpredictable insulation surface flashover in pressurized SF6," J. Phys. D: Appl. Phys., doi.org/10.1088/1361-6463/abb38f, 2020.
[20] M. Tahara *et al*, "Charge Accumulation Properties in Saturated and Aromatic Hydrocarbons by Electron Beam Irradiation," *Annu. Rep. Conf. Electr. Insul. Dielectr. Phenom. (CEIDP)*, 2008, pp. 165–168.
[21] M. Meunier and N. Quirke, "Molecular modeling of electron trapping in polymer insulators," J. Chem. Phys., vol. 113, no. 1, pp. 369–376, 2000.
[22] M. A. Baferani *et al,* "Interfacial charge dynamics in multi-dielectrics under various electric fields and thermal gradient," *IEEE Electr. Insul. Conf. (EIC)*, 2020, pp. 474-477.
[23] G. Mazzanti *et al*, "Apparent trap-controlled mobility evaluation in insulating polymers through depolarization characteristics derived by space charge measurements," J. Appl. Phys., vol. 94, no. 9, pp. 5997–6004, 2005.
[24] G. Mazzanti, G. C. Montanari, and J. M. Alison, "A space-charge based method for the estimation of apparent mobility and trap depth as markers for insulation degradation-theoretical basis and experimental validation," IEEE Trans. Dielectr. Electr. Insul., vol. 10, no. 2, pp. 187–197, Apr. 2003.
[25] G. Teyssedre and C. Laurent, "Charge transport modeling in insulating polymers: from molecular to macroscopic scale," IEEE Trans. Dielectr. Electr. Insul., vol. 12, no. 5, pp. 857–875, Oct. 2005.

Mohamadreza Arab Baferani received the BSc degree of electrical engineering from Iran University of Science and Technology, Iran and MSc from University of Tehran, Iran. Currently, he is a PhD candidate of electrical engineering and graduate research assistant at University of Connecticut. His main research interests are high voltage engineering, HVDC cable systems, composite polymeric insulations, and fault current limiters.

Chuanyang Li received his double B.S. degrees of electrical engineering and English from Taiyuan University of Technology. After that, he spent 3 years to obtain his M.S. degree from the Department of Electrical Engineering, Taiyuan University of Technology, from 2011 to 2014. He received his Ph.D degree in the Department of Electrical Engineering, Tsinghua University in 2018. He then worked as a Postdoctoral Fellow at the Department of Electrical, Electronic and Information Engineering "Guglielmo Marconi" of the University of Bologna (Alma Mater Studiorum - Università Di Bologna), Italy from 2018 to 2019. He is currently working in the Department of Electrical and Computer Engineering & Institute of Materials Science, University of Connecticut, as a Postdoctoral Fellow. His research interests include surface charge behavior and modification methods and PD properties of high temperature material in harsh conditions. He served as the Lead Guest Editor of the IEEE Trans. Dielectr. Electr. Insul. Special Issue on Advanced Dielectrics for Gas-Insulated Transmission Lines in 2018, IOP Nanotechnology Focus Collection on Focus on Gas-Solid Interface Charging Physics in 2020, and the Guest Editor in High Voltage Special Issue on Interface Charging Phenomena for Dielectric Materials. He is an associate editor of IET High Voltage. He can be reached at lichuanyangsuper@163.com.

Tohid Shahsavarian was born in East Azerbaijan, Iran in 1989. He received the B.Sc. degree of electrical engineering from the University of Tabriz in 2011, and the M.Sc. degree from University of Science and Technology, Iran, in 2013. Then, he worked in the Department of Transmission and Distribution in Monenco Iran Consulting Engineers Company. He is currently working towards his Ph.D. degree in electrical engineering at University of Connecticut. His research interests include partial discharge analysis and risk assessment of AC and DC power cables, reliability analysis of HVDC grids, and geomagnetic disturbances.

JoAnne Ronzello is a research specialist at the Institute of Materials Science/Electrical Insulation Research Center at the University of Connecticut. JoAnne has spent more than 35 years working in the area of dielectrics including high voltage testing, failure analysis, dielectric spectroscopy, and novel experimental development. She holds undergraduate degrees in chemistry and electrical engineering.

Yang Cao graduated with B.S. and M.S. in physics from Tongji University in Shanghai, China, and received his PhD from the University of Connecticut in 2002, after which he served as a senior electrical engineer at GE Global Research Center until 2013. He is currently a professor at the Electrical and Computer Engineering Department of the University of Connecticut. Dr. Cao is also the Director of the Electrical Insulation Research Center, Institute of Materials Science and the Site Director of the NSF iUCRC Center on High Voltage/Temperature Materials & Structures. His research interests are in the physics of materials under extremely high field and the development of new dielectric materials, particularly the polymeric nanostructured materials, for energy efficient power conversion and renewables integrations, as well as for novel medical diagnostic imaging devices.